CHAPTER-6

Design and Analysis of Magnetorheological Damper-based Ankle-Foot Prosthesis Prototype

Highlights of the Chapter

- *Ankle-foot prostheses prototype*
- *Magnetorheological damper control*
- *Analysis of model using ANSYS Software*

ABSTRACT

Purpose – This chapter highlights the design of a magnetorheological damper and a 3D printer technology-based powered ankle-foot prosthesis.

Design/methodology/approach – A prototype is proposed for the ankle-foot prostheses using the following components: magnetorheological damper, digital servomotor, encoder DC servomotor, 3D- printed parts of ABS material, etc. The CAD model of the prosthetic foot, leaf spring, retention spring, and connecting parts between the pylon and damper actuator assemblies are designed. 3D CAD design software such as CATIA and Solidworks is used for this purpose. Fused deposition modeling 3D printer-based technique is used for printing the parts using ABS filament. The first part of the prototype controls the magnetorheological actuator that absorbs the impacts during walking. The second part generates dorsiflexion and plantarflexion movements through the control of the electric actuator. The designed prototype is then tested on a transtibial amputee under a prosthetist's supervision.

Findings – Observations from ANSYS software-based analysis show that the prototype is safe from mechanical failure. It has safety factor values between 4.7 and 8.7 for heel strike, mid-swing, and toe-off. Upon testing the prototype on the amputee for a level ground walk, the amputee found it comfortable compared to the passive prosthesis.

Originality/value – The design of the prototype presented in the chapter has a better dynamic range for locomotion than passive prosthesis along. It also seems key to diminish injuries and give relief to the transtibial amputees.

6.1 Introduction

As per the Census of India 2011, out of 121 crores, 2.68 crores population are disabled. Out of the above number, about 20% have an impairment related to mobility (Verma *et al.*, 2016). The major cause of lower limb amputation can be linked to increased accidents and the spread of diabetes. Amputation is a traumatic process, and out of 91.7% of lower limb amputations, 53% are transtibial and 33% transfemoral (Masum *et al.*, 2014). The development of lower-limb prosthetic devices in developing countries like India has to factor in the below-average income of people. Thus, it is essential that the device has to be low-cost while providing proper human mobility.

The three types of prosthetic feet are conventional feet (CF), energy-storing-and-returning (ESR) feet, and bionic feet. Versluys *et al.* (2009) have presented the state-of-the-art review of passive TT prostheses covering CF and ESR feet. As the passive devices cannot provide ankle power during gait, there has been a surge in incorporating active elements in prosthesis design. Based on the speed of walking, the human ankle shows both passive and active behaviors (Shultz *et al.*, 2014). One crucial characteristic of any prosthetic device is an adaptation to any terrain. It cannot be achieved using a passive prosthesis. The research has been widely impacted by the recent developments in high-performance brushless DC motors, low-cost energy-efficient batteries, microcontrollers, and on-chip inertial measurement units (IMUs) (Lawson *et al.*, 2014). Most prostheses require heavy actuators to supply propulsion power which in turn improves the amputee's walking experience.

An active prosthesis is powered using batteries, while the passive ones use the user's power for actuation. Various actuators used in the existing prostheses are DC motors, brushless DC (BLDC) motors, servo motors, and AC motors (Weerakkody *et al.*, 2017). The proposed model employs two parts, one for absorbing the impacts during walking and the other for dorsiflexion and plantarflexion movements. Different parts of the ankle-foot prosthesis were designed in the CAD software and later simulated in the ANSYS software for the 3- positions of a stride by applying a load of 1000N.

6.2 Material and Methods

This section highlights available foot prostheses along with the concept of magnetorheological damper and its specifications and control. Finally, the working of the prosthesis prototype is explained. The amputee in current research has a K level of 3 and can move with variable cadence. The age of the transtibial amputee is 32 years. He lost his leg 11 years ago and has a height and weight of 168 cm and 70 Kg, respectively. The amputee has given his consent before trial, and the institute's ethical committee approves the study. The workflow used in the present study to design a powered ankle-foot prosthesis is as below: design of model using CAD tool; analysis of foot for different positions; analysis of leaf spring; fabrication of Acrylonitrile Butadiene Styrene (ABS) material-based 3D printed parts and stainless-steel (SS) leaf springs; control of MR damper; control of DC servo motors; setup installation on an amputee; and feedback from the amputee. Figure 6.1 shows the workflow diagram to control an ankle-foot prosthesis prototype.

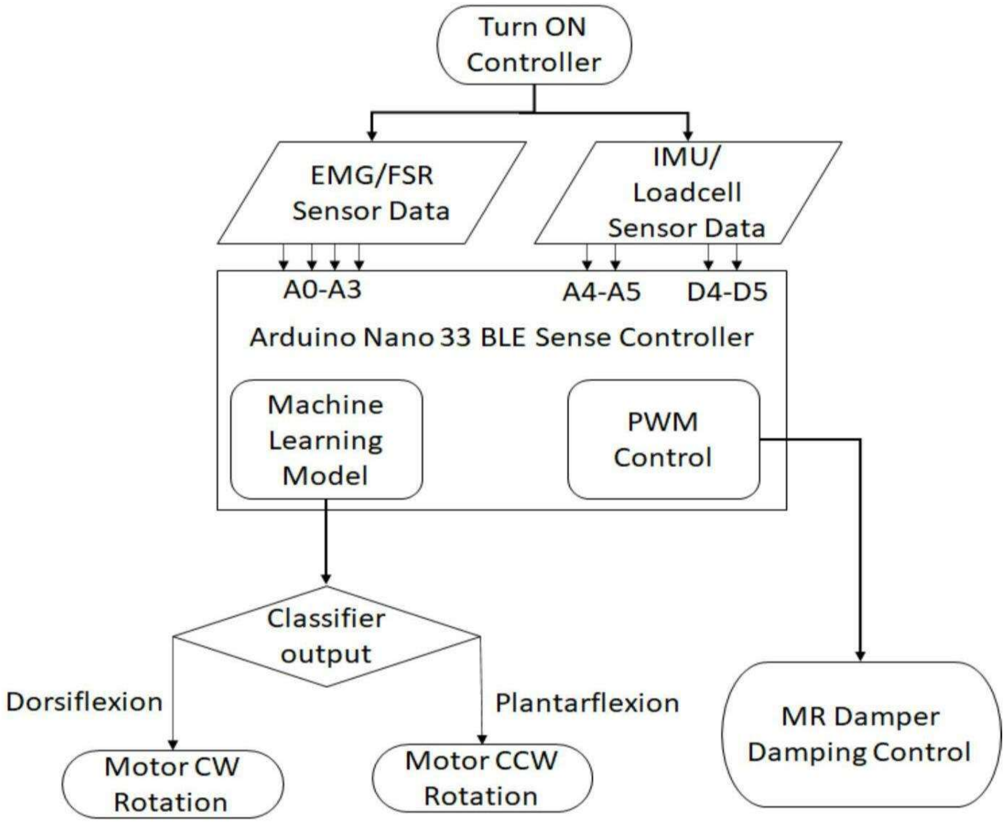

Figure 6.1 *Workflow diagram for Arduino based ankle-foot prosthesis control*

6.2.1 Ankle-Foot Prosthesis Models

To initiate the design of any prosthesis, knowledge of biomechanics and limb anatomy is crucial. (Winter, 2009). The term "gait cycle" describes the time duration from one heel-strike (HS) to another HS of the same foot. One gait cycle consists of stance and swing phases, divided into 8 subphases (Perry and Davids, 1992). The inclusion of a number of subphases to provide controlled damping in the prototype design is at the researcher's discretion. In this section, the technology used by various authors is presented.

Au *et al.* (2008) used controlled plantarflexion, controlled dorsiflexion, powered plantarflexion, and swing phases to study the gait cycle for level-ground walking. Sup *et al.* (2008) used a slider-crank mechanism to drive the lower limb joints using two motor-driven ball screw elements. Eilenberg *et al.* (2010) used the simulation on ankle plantar flexors with positive force feedback to control muscle reflex. To make the amputees' walking gaits more stable and natural, Zhu J. *et al.* (2010) introduced foot-prosthesis with Powered Ankle and Toe Joints (PANTOE). Later Yuan *et al.* (2011) presented a finite-state control strategy for PANTOE. Parsan and Tosunoglu (2012) divided the gait cycle into four segments, each with different mathematical expressions to control output foot angle value. A series of powered transtibial prostheses (AMP-Foot 2 and 3) is presented by Cherelle *et al.* (2013, 2016). AMP-Foot 3 used two locking mechanisms instead of a low-power actuator in AMP-Foot 2 to improve actuation.

Shultz *et al.* (2013, 2014) worked on a level walking controller for a powered ankle prosthesis prototype, and evaluation was done on a healthy subject using the able-bodied adapter for treadmill walk. In their study, the ankle behavior is partitioned into four essential functions in a stride. The model provides the damping during the late swing and HS, and the foot is stiff during the middle stance. During push-off, it gives power, and finally, the ankle angle becomes neutral during the swing. Ficanha *et al.* (2014b) presented a powered ankle-foot prosthesis that features the turning and walking on a straight path using a cable-driven multi-axis. Caputo and Collins (2014) developed an experimental platform for a tethered ankle-foot prosthesis incorporating an off-board motor and control system. However, the utilization of a 1.61 kW AC servomotor with planetary gear, embedded velocity control motor drive, and a controller (ACEl 103, dSPACE Inc., Wixom, MI) make such a system too costly, also not suitable to make a standalone system to carry with amputee while walking.

Kannape and Herr (2014) acquired the myoelectric signal from the residual limb muscles to aid the amputee during stair-ambulation. The electrodes' positions are determined by the palpation method, and these muscles are dorsiflexor and plantar flexor muscles. Young *et al.* (2014) used the combination of electromyography (EMG) and mechanical sensors data for locomotion mode recognition in transfemoral amputees. Other prostheses are instrumented with load cells to measure the ground reaction force (GRF), a potentiometer for ankle angle, and IMU sensors to detect shank and foot tilt angle (Chen *et al.*, 2014). An ideal prosthesis must have the following characteristics: (1) ability to generate net power during locomotion, (2) minimal energy consumption, and (3) weight and height less than that of a lost limb (Martinez *et al.*, 2014). The authors used a *60 Watts* brushless Maxon DC motor to drive a ball-screw via a timing belt. The ball screw was coupled with Ossur®, *Flex foot,* to emulate a human foot's function.

To design a prosthetic foot fused deposition modeling (FDM), 3D printing is used. The raw materials include Acrylonitrile Butadiene Styrene (ABS), polylactic acid (PLA), and carbon fiber reinforced PA6 (Nylon 6) filaments. The finite element (FE) analysis tool helps determine the stress and strain characteristics in the lower limb prosthesis (Tao *et al.*, 2017).

6.2.2 Magnetorheological Damper: Application in Lower-Limb Prosthesis

The damping force in a gait cycle changes based on flexion angles and other forces. (Nordin *et al.*, 2018). The special fluid used in the damper is called magnetorheological fluid. It can change its rheologic properties according to changes in the magnetic field. Nandy *et al.* (2012) used the MR damper to control an above knee amputee's knee movement. The stiffness of the MR Damper is controlled through a PWM controller based on HS pressure. MR knee prosthesis proposed by Pandit *et al.* (2018) adjusts the damping using the knee force, torque, and position sensor data. Tyan *et al.* (2009), using

RecurDyn with Simulink package, demonstrated the effectiveness of a semiactive controller for an above-knee prosthesis with an MR damper. Below-knee prosthesis augmented with an MR Damper enhances comfort for the amputee while improving the dynamic range.

Arteaga *et al.* (2019) proposed a prototype for robotic ankle-foot prosthesis using MR fluids-based damping to perform dorsiflexion and plantarflexion actions. 100kg Uxcell extensometer gauge and Two FSR402 sensors on a prosthetic foot sole acquire the damping force data. The PWM signal is calculated using the Arduino Nano board and is sent to a TB6612FNG motor driver that controls the damping parameters according to the required force. An amputee can avail complete gait kinematics along with real-time gait phase detection and control using just a single damper. In the previous study, the authors have presented real-time gait phase detection using FSR and IMU sensors (Negi *et al.*, 2021). FSR and IMU sensors provide necessary information for normal gait kinematics; the EMG signal indicates the muscle activation at different gait phases, enabling the MR damper's current control during the different phases of a gait cycle. It forms the basis for the design of a simple MR damper-based ankle-foot prosthesis.

6.2.3 MR Damper Specifications

Table 6.1 highlights the mechanical and electrical specifications of the MR damper. Typical performance characteristics of the MR damper are displayed in Figure 6.2, which uses a force-velocity curve. The curves are mentioned for different values of the current passed through the damper. The main idea to choose this damper for prosthetic application is its actuation time; it alters damping within a fraction of seconds.

Table 6.1 *MR damper specifications*

Shock absorber type	Adjustable compression and tension
Damper type	Linear
Extended length	180 mm
Compressed length	137.5 mm
Stroke length	42.5 mm
Damping force	< 240 N, 0.13m/s @ 0A > 1400 N, 0.39m/s @ 2.5A
Input voltage	0-15 V DC
Input current	0 – 3 A
Resistance at ambient temperature	5 – 5.3 Ohm Approx.

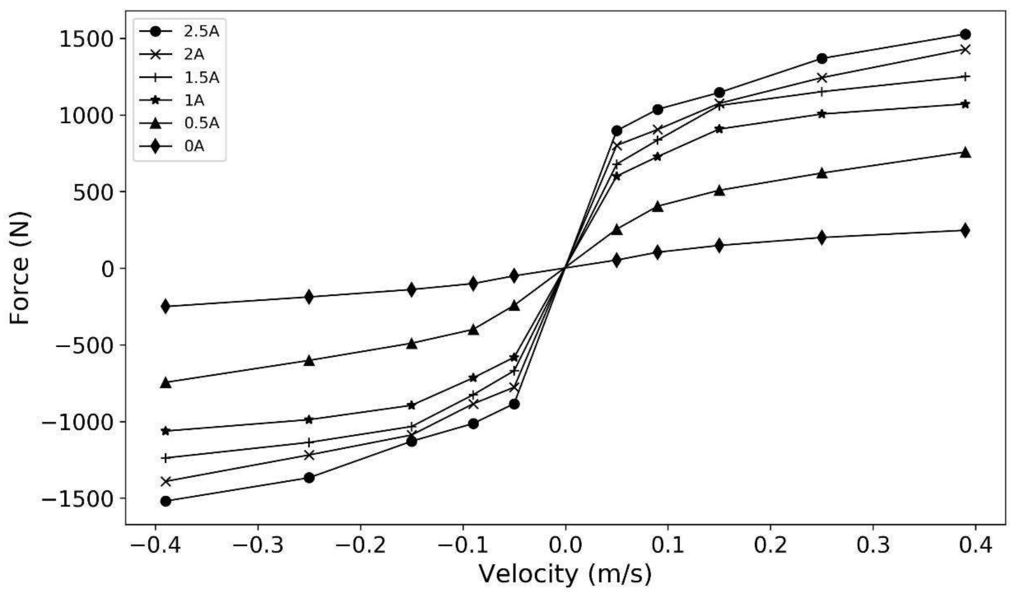

Figure 6.2 *Force-velocity curve for MR damper*

6.2.4 MR Damper Controller

As the electrical current passes through the MR damper, a coil inner to the piston produces a magnetic field and instantly modifies the piston's MR Fluid properties; accordingly, the damping is altered in real-time, controlling the electrical current to the damper. The control circuit used in the present study consists of an Arduino Nano processor, P channel MOSFET, MOSFET gate driver IC, inductor, capacitor, and diodes. Figure 6.3 shows the schematic of the circuit designed for this study. For controlling the MR damper current, the voltage across it needs to be varied. Considering the MR damper resistance value of 5 ohms, the input voltage of 0-10 volts gives 0-2 amperes at the output. Therefore, a converter is required to vary the output voltage between 0-10 volts effectively. A DC-to-DC buck converter circuit is designed that uses a DC supply from an 11.1V lithium-polymer (Li-Po) battery. Arduino Nano controls the PWM signal fed to MOSFET gate driver IC TC4427 which drives the IRF5210 P channel MOSFET used as a switch; thus, Arduino controls the PWM voltage at its gate.

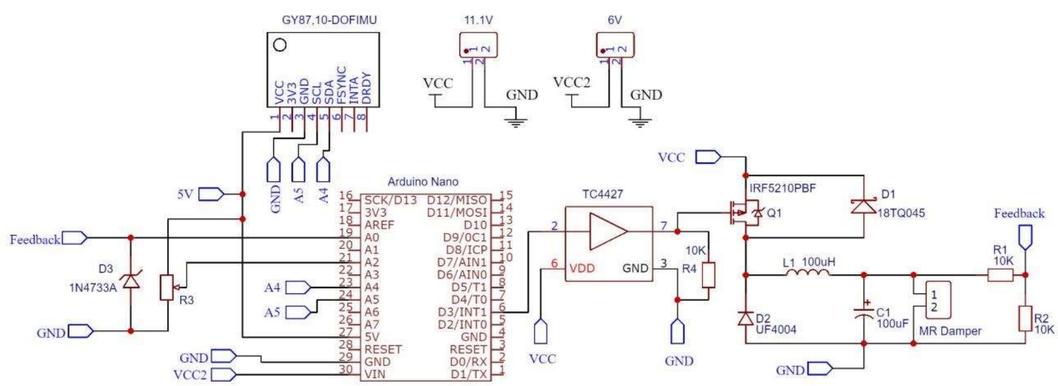

Figure 6.3 *Circuit for Arduino Nano-based MR damper control*

IMU connections are provided in the printed circuit board (PCB), providing vertical linear acceleration data while walking. To manually control the MR damper, a potentiometer is attached to the board's A2 pin, and the analog input is converted to a relative PWM count, which further controls the MOSFET. Authors also provided an option for feedback voltage achieved using a potential divider at MR damper's output, where a maximum output voltage say (10 volts) becomes half (i.e., 5 volts); that is fed to the Arduino Nano input pin A0, which is in the safe limit of 5 volts. A 5.1-volt Zener diode is connected between A0 and GND to protect the Arduino against overvoltage. The 2-D view of the designed PCB and schematic diagram is shown in Figures B.3 and B.4.

For the initial study, the simulation was performed in Proteus Design Suite [Labcenter Electronics Ltd] software by assuming the resistance of MR Damper as 5 ohms while manually varying the potentiometer value. By dividing potentiometer readings into 10 different input voltages ranges, the output current is controlled according to 10 PWM levels.

Table 6.2 *MR damping control using a Potentiometer*

Potentiometer Reading (after mapping)	PWM value	Damper Current (in Amperes)
> 225 && <= 255	25	1.98
> 200 && <= 225	50	1.74
> 175 && <= 200	75	1.51
> 150 && <= 175	100	1.28
> 125 && <= 150	125	1.05
> 100 && <= 125	150	0.82
> 75 && <= 100	175	0.59
> 50 && <= 75	200	0.37
> 25 && <= 50	225	0.17
>= 0 && <= 25	255	0

Figure 6.4 shows the output voltage and current values of the MR damper circuit for three positions of potentiometers: (a) 0%, (b) 29%, and (c) 100%. The variable damping in different gait phases is achieved by varying the current for each sub-phase. Another way of achieving variable damping involves using an IMU sensor on the rear part of the foot. The vertical acceleration values obtained from the IMU sensor can be mapped to

continuous PWM values to achieve proportionality in current. The introduction of semi-active damping was found to be comfortable for the amputee.

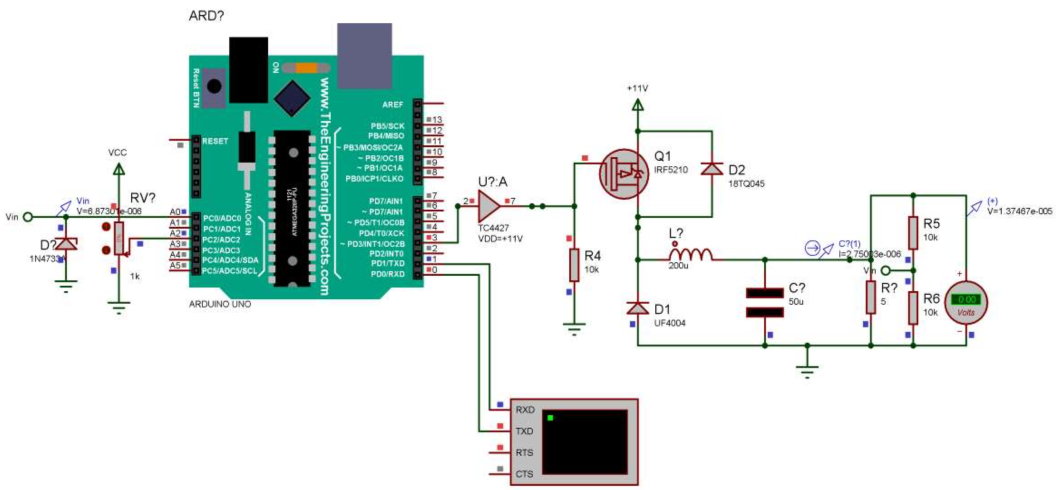

(a)

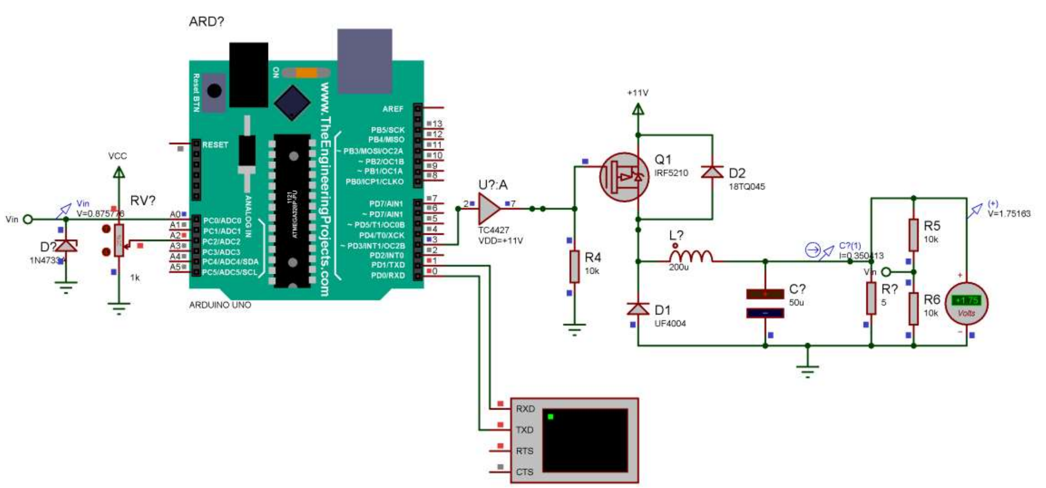

(b)

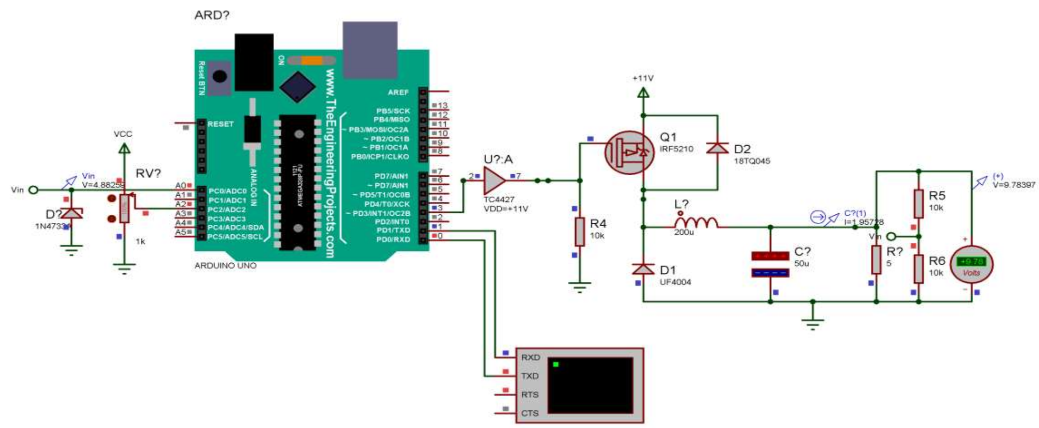

(c)

Figure 6.4 *Voltage and current output of MR damper circuit for 3 different positions of potentiometer: (a) 0%, (b) 29%, and (c) 100%*

6.2.5 Prototype Working

When an individual loses a body part due to an accident or agenesis, introducing a prosthesis improves the quality of life. A prosthesis aims to artificially replace the lost body part while also enabling partial or complete function of the original part. The authors presented two prosthesis models in Figure 6.5 and simulated the response to static load using ANSYS software. The essential components of a below-knee (BK) prosthesis are the ankle-foot, leg, socket, and suspension system. The base foot and connecting frames are 3D printed using ABS filament. The leaf spring and extension springs are made of AISI 1035 Steel (SS) material.

An MR damper is attached at the rearfoot that is connected to the pylon through connecting frames. A servo motor, leaf spring, and extension springs attached to the connecting frame on the front side of one mechanism actuate the foot during the swing phase to make proper heel strike, and it also supports during the dorsiflexion and plantarflexion of the foot. During the HS event, the damping force counteracts the heel's ground reaction force by driving maximum current through damper to absorb shock, while during foot flat, the damping force is reduced due to fall in current. During TO, the MR damper's stroke length is minimum; therefore, the damping is soft during this phase.

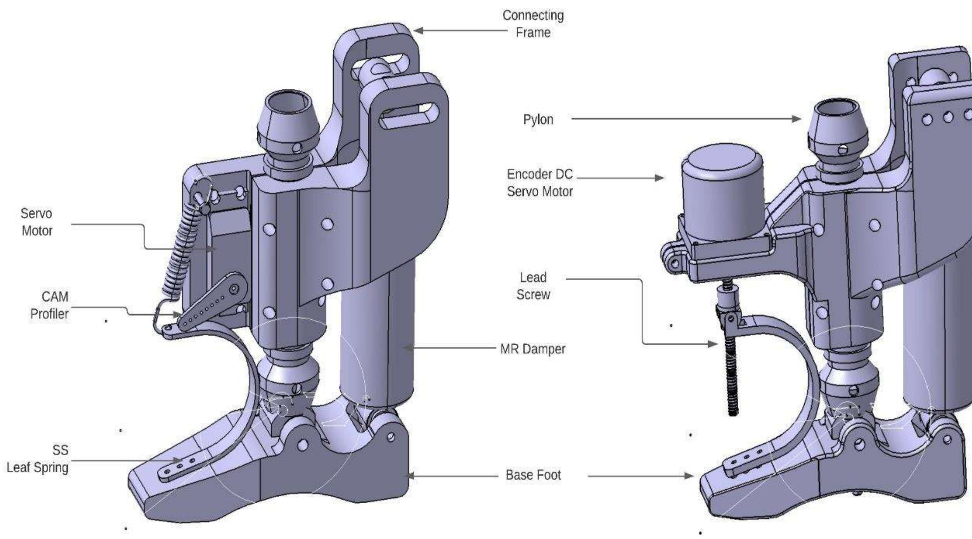

Figure 6.5 *CAD models for prosthetic foot prototypes*

Alternatively, a lead screw can be coupled with a servo motor to control the dorsiflexion or plantarflexion of the foot by rotating the motor in clockwise (CW) or counter-clockwise (CCW) direction respectively. During heel strike, the damper is active; at mid-stance, the motor rotates to zero position, and during TO, the damper is inactive to perform foot movements. In the swing phase, the motor is rotated CW to turn the foot from plantarflexion to dorsiflexion so that the heel strikes the ground on the next HS event.

The best muscles for generating intent-based signals are the tibialis anterior, medial gastrocnemius muscles, lateral gastrocnemius muscles, and peroneus muscles. The foot's dorsiflexion and plantarflexion are controlled using the TinyML algorithm in Arduino Nano BLE 33 Sense controller. The control signals relative to gait events can also be generated using other sensors like a potentiometer, wearable IMU, and FSR sensors.

Figure 6.6 shows the HS, mid-stance, TO events for an amputee walking on MR damper-based ankle-foot prosthesis model prototype.

Figure 6.6 *Transtibial amputee walking on MR damper-based ankle-foot prosthesis prototype*

6.3 RESULTS AND DISCUSSION

To ensure the failsafe design of the prosthetic foot, it was first analyzed in ANSYS WORKBENCH. The foot was tested by gradually introducing a constant load with time. This analysis helps in reducing failure chances in actual-life conditions. A mesh-convergence graph of stress against mesh size is used to balance the analysis accuracy and computational time to validate the results. Mesh size with less than 5% error to the succeeding value of stress is chosen, which came out to be 2mm.

6.3.1 Prosthetic Foot Analysis

A force of 1000N at varying angles was tested for each gait event. For HS, the force is applied from the ground at an angle of 20 degrees from the horizontal on the prosthetic foot's rear part while keeping the ankle restricted to 5 degrees of freedom (3 translational, 2 rotational), as shown in Figure 6.7. For mid-stance, a force from the ground is applied perpendicular to the surface of the foot, as shown in Figure 6.8.

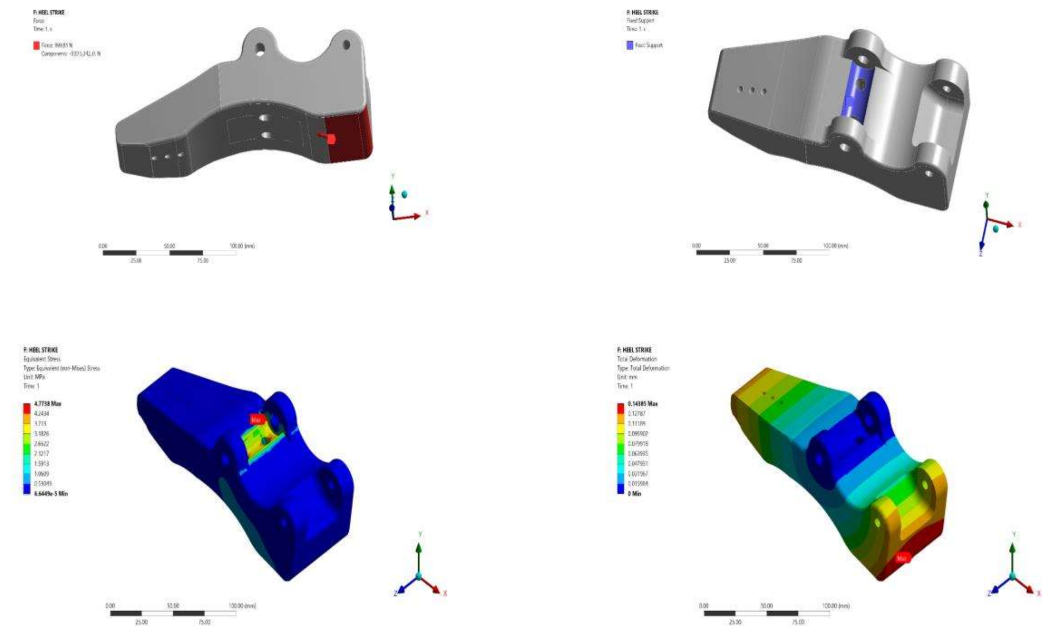

Figure 6.7 *Analysis of Prosthetic foot prototype during heel strike*

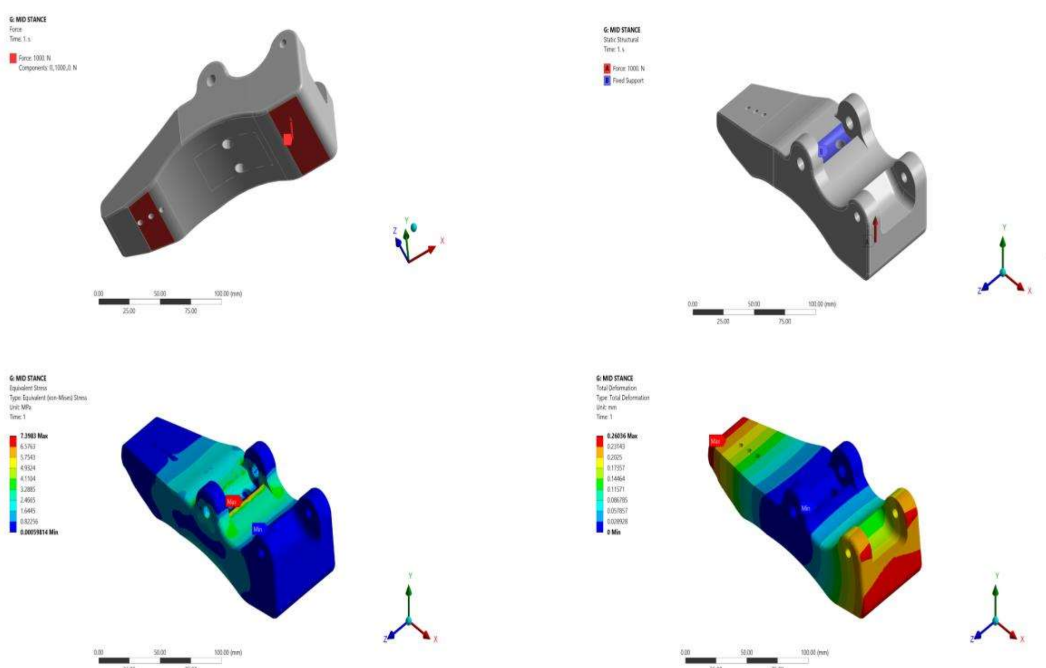

Figure 6.8 *Analysis of Prosthetic foot prototype during mid-stance*

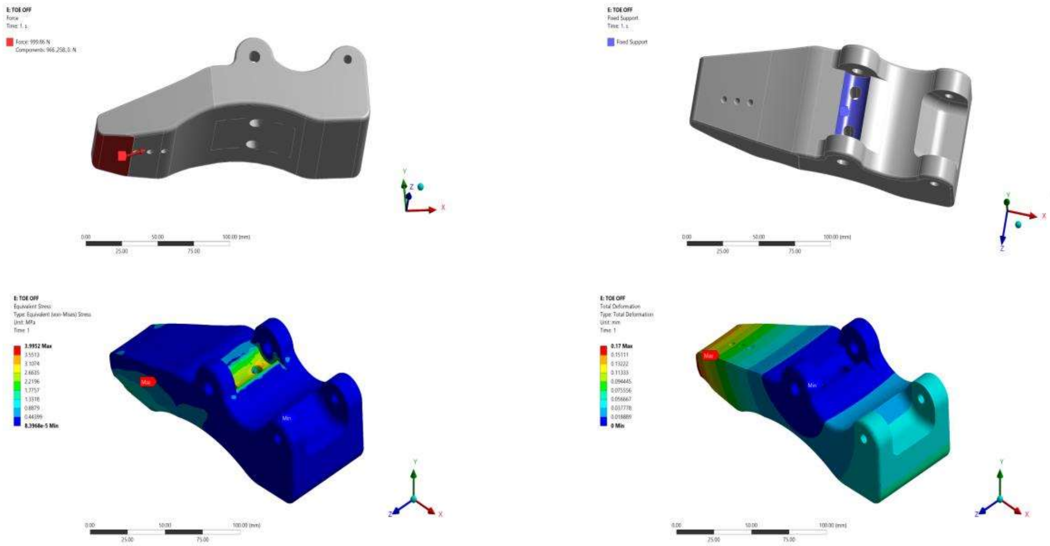

Figure 6.9 *Analysis of Prosthetic foot prototype during toe-off*

For TO, the force is applied from the horizontal plane at an angle of -15 degrees, as demonstrated in Figure 6.9. The yield stress of ABS filament varies from 20 to 50 MPa; in the analysis, the authors assumed a mean value of 35 MPa. Table 6.3 highlights the results in the tabular form for three-foot positions.

Table 6.3 *Analysis results for different foot positions*

Foot Position	Yield Stress (MPa)	Maximum Stress (MPa)	Total Deformation	Factor of safety (FOS)
Heel-strike	35	4.7738	0.14 mm	7.33
Mid-stance	35	7.3983	0.26 mm	4.73
Toe-off	35	3.9952	0.17 mm	8.76

6.3.2 Leaf Spring Analysis

Leaf spring experiences the force transmitted by the cam attached to a 60 kg-cm motor. A gradual load upto 100N is applied and there is line contact between cam and leaf spring, as shown in Figure 6.10. Another end of the spring was fixed from all 6 degrees of freedom. It is essential to regularly check for the life of leaf spring under stress as it is prone to fatigue due to repeated loading and unloading cycles. The loading is a zero-based reverse load. GERBER criterion (Rawal *et al.*, 2016; Truong and Nguyen, 2021) is used for fatigue failure due to the ductile nature of leaf spring material.

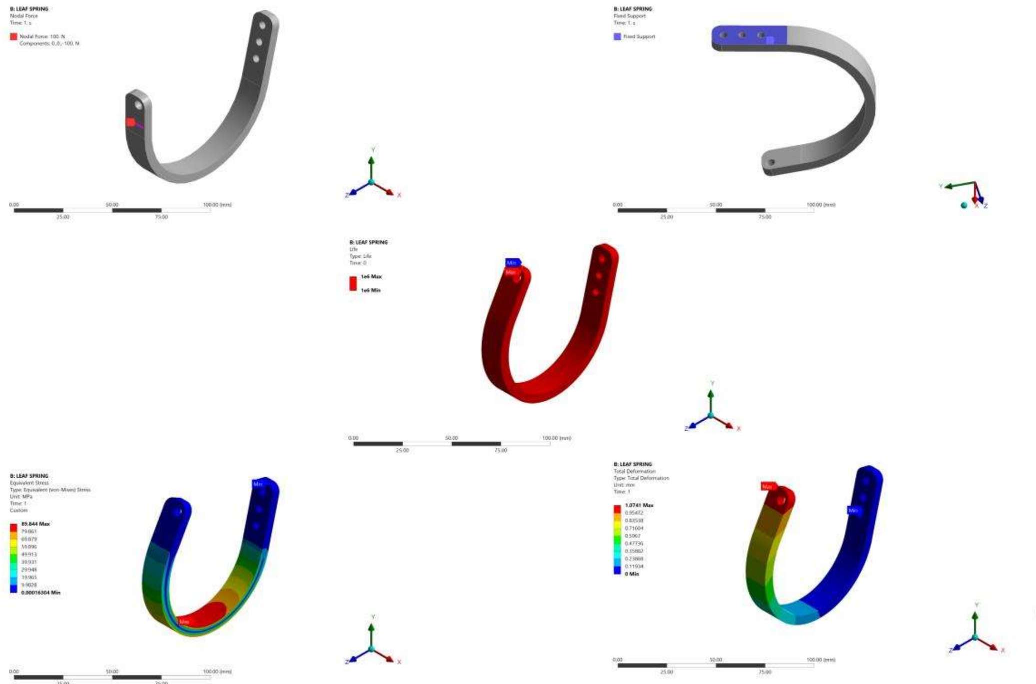

Figure 6.10 *Analysis of leaf spring*

6.3.3 A Summary of Amputation and Prosthesis Design

The entire process of prosthesis design and fabrication was conducted in the institute laboratory and tested on a K3 level amputee (can ambulate with variable cadence) in the prosthetic center under the supervision of a prosthetist. Few parts such as pylon, pyramid adapter, leadscrew, and DC servo motors were purchased online from the Indian market. The MR damper was ordered explicitly from Arus MR Tech Pvt Ltd, Chennai, India, at 26,300 INR; bulk orders may reduce this cost. The approximate cost for the proposed ankle-foot prosthesis prototype is 22,000 INR, excluding the MR damper. The total weight of the prosthesis prototype is 3kg that can be reduced by designing a lightweight

MR damper and using a carbon fiber-based pylon. A summary of amputation and prosthetic design is presented in Table 6.4.

Table 6.4 *A summary of amputation and prosthesis design*

Amputation level	K3
Stump length	9 inches
Prosthesis weight	3.00 Kg (including Battery and MR damper)
Prosthesis height	0.28 m
Max. allowable dorsiflexion/ plantarflexion (for 1.2s gait cycle)	For 80 mm distance between the pylon and lead screw axes 6.5 deg [300 rpm DC servo motor] 13.5 deg [600 rpm DC servo motor] 20 deg [900 rpm DC servo motor]
	For 50 mm distance between the pylon and lead screw axes 11 deg [300 rpm DC servo motor] 22 deg [600 rpm DC servo motor] 34 deg [900 rpm DC servo motor]
Battery	5200 mAh 3S 40C Li-Po
Cost	22000 INR (excluding MR damper)

6.4 Conclusion

A working prototype of an ankle-foot prosthesis was presented that includes an MR damper to make it semi-active. The mean yield stress of ABS foot material is almost 35 MPa. Result analysis showed that the actual stress is way less than the yield stress in all the components, which achieved a high factor of safety values. Also, the deformation in the components is negligible. Hence, it may be concluded that the prosthetic foot model components are safe from all forms of mechanical failure. For leaf spring, since it is under cyclic loading during the gait cycle, its fatigue analysis showed that it could endure $10^{\wedge 6}$cycles, i.e., it has infinite life. Hence it is also safe from failure. The ankle-foot prosthesis prototype is tested with an MR damper on an amputee; he felt comfortable walking by wearing it compared to his passive prosthesis. It is concluded that after the proper selection of actuator components, the prototype may be adopted on BK amputees as per the specification of amputees.